

UDC 621.371

doi:10.31799/1684-8853-2019-3-94-104

## Optical data signals in fiber optic communication links with fading

I. Juwiler<sup>a</sup>, PhD, Senior Lecturer, [orcid.org/0000-0002-0669-7828](https://orcid.org/0000-0002-0669-7828)

I. Bronfman<sup>a</sup>, Assistant, [orcid.org/0000-0001-6195-069X](https://orcid.org/0000-0001-6195-069X)

N. Blaunstein<sup>b</sup>, Dr. Sc., Phys.-Math., Professor, [orcid.org/0000-0003-2945-9379](https://orcid.org/0000-0003-2945-9379),  
[nathan.blaunstein@hotmail.com](mailto:nathan.blaunstein@hotmail.com)

<sup>a</sup>Electrical and Electronics Engineering Department, Shamoon College of Engineering, 84, Jabotinsky St., Ashdod, 77245, Israel

<sup>b</sup>Ben-Gurion University of the Negev, P.O.B. 653, 1, Ben-Gurion St., Beer-Sheva, 74105, Israel

**Introduction:** This article is based on the recent research work in the field of two subjects: signal data parameters in fiber optic communication links, and dispersive properties of optical signals caused by non-homogeneous material phenomena and multimode propagation of optical signals in such kinds of wired links. **Purpose:** Studying multimode dispersion by analyzing the propagation of guiding optical waves along a fiber optic cable with various refractive index profiles of the inner optical cable (core) relative to the outer cladding, as well as dispersion properties of a fiber optic cable due to inhomogeneous nature of the cladding along the cable, for two types of signal code sequences transmitted via the cable: return-to-zero and non-return-to-zero ones. **Methods:** Dispersion properties of multimode propagation inside a fiber optic cable are analyzed with an advanced 3D model of optical wave propagation in a given guiding structure. The effects of multimodal dispersion and material dispersion causing the optical signal delay spread along the cable were investigated analytically and numerically. **Results:** Time dispersion properties were obtained and graphically illustrated for two kinds of fiber optic structures with different refractive index profiles. The dispersion was caused by multimode (e.g. multi-ray) propagation and by the inhomogeneous nature of the material along the cable. Their effect on the capacity and spectral efficiency of a data signal stream passing through such a guiding optical structure is illustrated for arbitrary refractive indices of the inner (core) and outer (cladding) elements of the optical cable. A new methodology is introduced for finding and evaluating the effects of time dispersion of optical signals propagating in fiber optic structures of various kinds. An algorithm is proposed for estimating the spectral efficiency loss measured in bits per second per Hertz per each kilometer along the cable, for arbitrary presentation of the code signals in the data stream, non-return-to zero or return-to-zero ones. All practical tests are illustrated by MATLAB utility.

**Keywords** — capacity, cladding, core, delay spread of optical pulses, dispersion curves, dispersion diagram of optical modes, fiber optic cable, graded-index cable, material time dispersion, linearly polarized (LP) modes, material dispersion factor, multimode time dispersion, non-return-to-zero (NRZ) code, numerical aperture, optical modes in cable, refractive index, relative refractive index, return-to-zero (RZ) code, single-mode condition, spectral efficiency, step-index cable.

**For citation:** Juwiler I., Bronfman I., Blaunstein N. Optical data signals in fiber optic communication links with fading. *Informatsionno-upravliaiushchie sistemy* [Information and Control Systems], 2019, no. 3, pp. 94–104. doi:10.31799/1684-8853-2019-3-94-104

### Introduction

In recent years there observed huge development of complex communication systems, including both radio and optical wired and wireless communication, mostly in the modern 4<sup>th</sup> and 5<sup>th</sup> generations of communication networks. This first of all related to growth demands to increase of the rate of information transfer, its density during transmission, as well as to exponential grow of number of subscribers — users of wired and wireless communication. In this case increases the role of wired optical communication — fiber optic guiding systems — optical cables. However, practice showed that such “wired” channels are affected by fading caused by multimode interference of modes propagating within the channel, which has stochastic character, as well as by inhomogeneous and roughness structure of cable walls, leading to deviations of propagating modes from specular reflection. Cumulatively, these phenomena lead to “spreading” of time delay of signals

along the fiber optical cable. These phenomena lead to dispersion of signals, and as the result — to loss of information transferred along the cable.

How much these phenomena lead to loss of information — nobody did not investigate systematically until nowadays. In the modern literature, only break empirical data were presented based on experimental observed data. However, was not developed unified unique approach to resolve the problem, which stimulated beginning of the problems investigations by the authors. Therefore, in the work from the beginning were introduced the optical cables that more been used in practice, with step-index and graded-index profiles of refraction indexes, analytically had considered character of propagation of optical waves (modes) inside the optical guiding structure, from which inhomogeneous structure of optical cable walls. As the result, spread of time delay of optical signals is shown depending on the type of coding of information inside them — return-to-zero or non-return-to-zero.

### Types of optical fibers

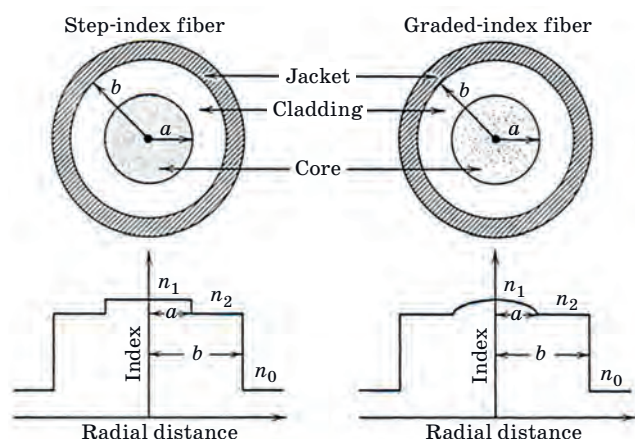
The first commonly used kind of fiber optic structure is the *step-index fiber* (Fig. 1).

The inner structure of each kind of fiber optic is schematically presented in Fig. 2.

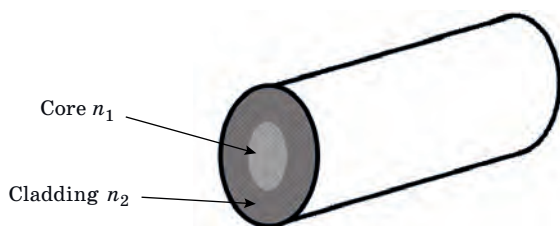
As it is clearly seen from Fig. 2, such kind of fiber consists of a central core of radius  $a$  and refractive index  $n_1$ , surrounded by a cladding of radius  $b$  and the refractive index  $n_2$ .

According to the definition of total intrinsic reflection (see definition in [1–3]), to obtain the total reflection from the cladding, its refractive index should be lower than that of the core, i. e.  $n_1 > n_2$ . Fig. 3 shows geometry of optical ray propagation within the core under the assumption that the cladding width is thick enough to exclude the evanescent field decay inside the cladding depth. So, from the beginning we can suppose that the effects of a finite cladding thickness are negligible, and a ray field is small enough to penetrate the outer edges of the cladding. As will be described below, in a multi-mode *step-index* fiber, a large modal distortion occurs.

To avoid such drawbacks of this kind of fiber, a new type, called *graded-index* fiber was developed [1–6] that has the same configuration as the previous fiber (shown in Fig. 1). The difference between both kinds of fiber is defined by differences in profiles of refractive indexes of core and cladding, as



■ Fig. 1. Difference between the refractive index profiles for step-index and graded-index fibers



■ Fig. 2. A view of the fiber optic inner structure

illustrated in Fig. 1. Thus, as clearly seen from illustrations, in the step-index fiber the index change at the core-cladding interface is abrupt, whereas in the graded-index fiber the refractive index decreases gradually inside the core.

In fiber optics, there is an important parameter that is usually used, called the *numerical aperture* of fiber optic guiding structure, denoted as N.A. [1–9]:

$$N.A. = n_1 \sin \theta_c \equiv \sin \theta_a,$$

where  $\theta_{full} = 2\theta_a$  is so-called in the literature as the angle of minimum light energy spread outside the cladding, or of full communication [10–14], when total internal reflection occurs in fiber optic structures. Accounting for  $\cos^2\theta = 1 - \sin^2\theta$ , we finally get

$$N.A. = (n_1^2 - n_2^2)^{1/2}.$$

Sometimes, in fiber optic physics, designers use the parameter, called the *relative refractive index difference* [1–9]:

$$\Delta = \frac{(n_1^2 - n_2^2)}{2n_1^2} \equiv \frac{(N.A.)^2}{2n_1^2}.$$

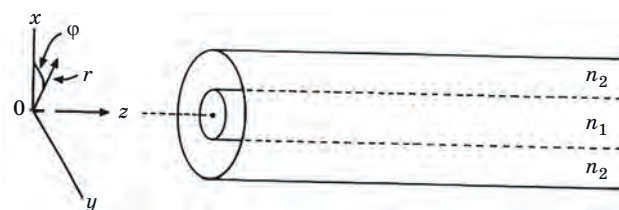
Using the above formulas, we can find relations between these two engineering parameters:

$$N.A. = \sqrt{2}n_1(\Delta)^{1/2}.$$

To understand the effects of optical wave propagation in both kinds of fibers, let us consider a similar 3D problem of ray propagation in a cylindrical waveguide, but now having more complicated geometry by having an inner core and an outer cladding.

### Propagation of optical waves inside the fiber-optic structure

Let us now consider the cylindrical dielectric structure as shown in Fig. 3. This is just the geometry of the optical fiber, where the central region is known as the *core* and the outer region as the *clad-*



■ Fig. 3. Presentation of fiber optic structure in the cylindrical coordinate system

ding. In this case, the same basic principles exist as for the dielectric slab, but the circular rather than planar symmetry changes the mathematics. We use the solution of Maxwell's equation in the cylindrical coordinates for both the coaxial cable and the circular waveguide, where we deal mostly with guiding modes rather than the ray concept [1–9, 13].

The wave equation that describes such propagation of light within cylindrical waveguides can be presented in cylindrical coordinates as follows for  $\mu_r = 1$ :

$$\nabla^2 E \equiv \frac{1}{r} \frac{\partial}{\partial r} \left( r \frac{\partial E}{\partial r} \right) + \frac{1}{r^2} \frac{\partial^2 E}{\partial \phi^2} + \frac{\partial^2 E}{\partial z^2} = \mu \varepsilon \frac{\partial^2 E}{\partial t^2}. \quad (1)$$

We can (as in [12–14]) present the solution by using the separation of variables:

$$E = E_r(r)E_\phi(\phi)E_z(z).$$

From well-known physics [10–14], we immediately take  $E_t(t)E_z(z) = \exp\{i(\beta z - \omega t)\}$ . This allows us to rewrite the wave equation (1) in the form

$$\frac{1}{r} \frac{\partial}{\partial r} \left( r \frac{\partial (E_r E_\phi)}{\partial r} \right) + \frac{1}{r^2} \frac{\partial^2 (E_r E_\phi)}{\partial \phi^2} - \beta^2 E_r E_\phi + \frac{n^2 \omega^2}{c^2} (E_r E_\phi) = 0.$$

We now suggest that function  $E_\phi$  is periodic and can be presented in the form

$$E_\phi = \exp(\pm im\phi),$$

where  $m$  is an integer. Now we can reduce the above equation as follows:

$$\frac{\partial^2 E_r}{\partial r^2} + \frac{1}{r} \frac{\partial E_r}{\partial r} + \left( n^2 \frac{\omega^2}{c^2} - \beta^2 - \frac{m^2}{r^2} \right) E_r = 0. \quad (2)$$

Equation (2) is a form of Bessel's equation and its solutions are Bessel functions [14]. We finally can obtain solutions for the field of rays through the modified Bessel functions of the first and second order,  $J(qr)$  and  $K(pr)$ , via wave parameters  $q$  and  $p$  as propagation parameters inside the core and cladding, respectively. This finally gives at the core ( $r \leq a$ )

$$\frac{\partial^2 E_r}{\partial r^2} + \frac{1}{r} \frac{\partial E_r}{\partial r} + \left( q^2 - \frac{m^2}{r^2} \right) E_r = 0$$

and at the cladding ( $r > a$ )

$$\frac{\partial^2 E_r}{\partial r^2} + \frac{1}{r} \frac{\partial E_r}{\partial r} + \left( p^2 + \frac{m^2}{r^2} \right) E_r = 0.$$

Solutions of these equations, respectively, are

$$E_r = E_c J_m(qr);$$

$$E_r = E_{c1} K_m(qr),$$

where  $J_m(qr)$  and  $K_m(qr)$  are the first kinds of the Bessel function; and the modified Hankel function (e. g., Bessel function of the second kind) [14], respectively. Roots of  $J_m(qr) \equiv J_m(v)$ ,  $m = 0, 1, 2, \dots$ , are shown in Fig. 4.

As for information of  $K_m(qr)$ , the reader can find it, for example, in [8, 9]. Finally, the full solution at the core is

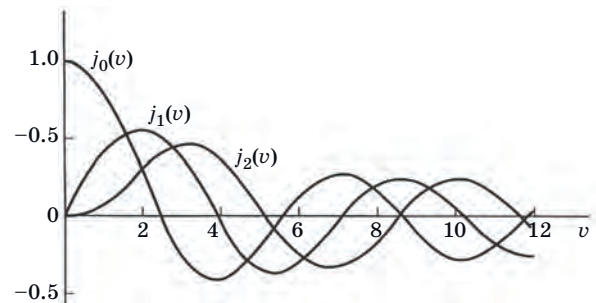
$$E = E_c J_m(qr) \exp\{-j(\omega t - \beta z)\} \exp(\pm jm\phi)$$

and a similar full solution for the cladding

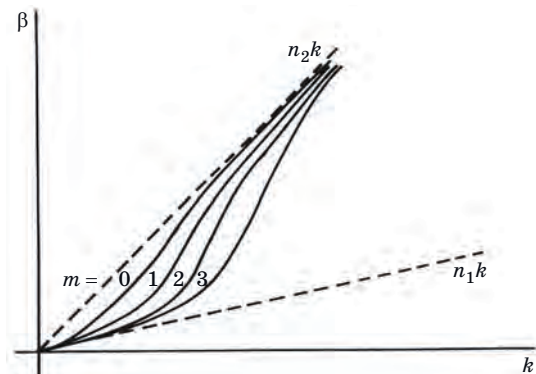
$$E = E_{c1} K_m(qr) \exp\{-j(\omega t - \beta z)\} \exp(\pm jm\phi),$$

where  $m$  is the azimuth integer.

Now, as in the case of the 3D cylindrical empty waveguide, described in [7], we can determine for an optical fiber the corresponding values for given propagation parameters  $k$  and  $\beta$ , by imposing the boundary conditions at  $r = a$ . The result is a relationship which provides the  $\beta$  versus  $k$  or *dispersion curves* shown in Fig. 5.



■ Fig. 4. Bessel function of the first kind and  $n$  order vs. variable  $v$



■ Fig. 5. Dispersion diagram of optical modes in a fiber optic structure

It is clearly seen that the modes with numbers from 0 to 3 (the same property occurring for modes with numbers  $n > 3$ ) propagate between the core and cladding of the fiber optic with wavelengths depending on refractive properties of these two fiber structures, and with an increase of wave propagation number  $k$ , propagate inside the inner (core) structure.

The full mathematical approach is very complicated, and we use the so-called “weakly guiding” approximation [12, 14]. This makes use of the fact that if  $n_1 \approx n_2$  the ray’s angle of incidence at the boundary “core-cladding” must be very large, if total internal reflection is to occur. The ray must bounce down the core almost at grazing incidence. This means that the wave is almost a transverse wave, with very small  $z$ -components.

Since the wave within the fiber is considered transverse, the solution can be resolved conveniently into two linearly polarized components, just as for free-space propagation. The modes are called *linearly polarized* (LP) [1, 2, 4]. All solutions obtained above relate directly to the optical fiber guiding structures. The latter has just the cylindrical geometry, and if for a typical fiber, we have that  $(n_1 - n_2)/n_1 \approx 0/01$  than the “weakly guiding” approximation is valid.

There are two possible LP optical fiber modes:  $LP_{01}$  ( $m = 0, n = 0$ ) and  $LP_{11}$  ( $m = 1, n = 1$ ) [1, 2, 4]. For cylindrical geometry, the *single-mode condition* is [12, 14]

$$\frac{2\pi a}{\lambda}(n_1^2 - n_2^2)^{1/2} < 2.404.$$

As follows from presented illustrations, depending on the shape of the intrinsic refractive index distribution, the corresponding LP-modes can propagate asymmetrically and inhomogeneously. This phenomenon is called the *modal dispersion* [1–9, 12–14] and will be discussed in the next section.

### Dispersion effects of signals occurring in fiber optic communication link

As was discussed in the previous paragraph, in fiber optic channels fading of optical signals occurs due to two factors: 1) multimode phenomena leading to the inter-ray interference and 2) dispersive properties of the material at the inner and outer coating of the fiber guide caused by inhomogeneous structure of the wire communication channel. Dispersion of these two types was discussed briefly in [9, 12, 14] and below in our description of the matter, we will follow on some of the formulas presented there.

A problem of transmission of pulses via fiber optic structure occurs because of two factors. One

is that the source of light is not emitted at a single wavelength, but exists over a range of wavelengths called the source spectral width [1–10]. The second factor is that the index of refraction is not the same at all wavelengths. The property of when the light velocity is dependent on the wavelength is called *dispersion*.

*Material Dispersion (MD)*. We can observe that the material dispersion is dependent on the properties of the material from which fiber structures are developed. Such a kind of dispersion caused the spread of the light wavelength as it travels along the fiber.

This is because each component wavelength (also called *wave harmonic*) travels at a different speed, each arriving with a slight delay with respect to the others. The amount of pulse spreading ( $\tau$ ) per unit of length of fiber ( $l$ ) is given by [12, 14]

$$\Delta\left(\frac{\tau}{l}\right) = -M\Delta\lambda,$$

where  $M$  is the *material dispersion factor*, and it is plotted in Fig. 6, according to [6, 7], for pure silica glass versus wavelength varied from 0.7  $\mu\text{m}$  in units of picoseconds per nanometer per kilometer [ps/(nm·km)] of length of fiber.

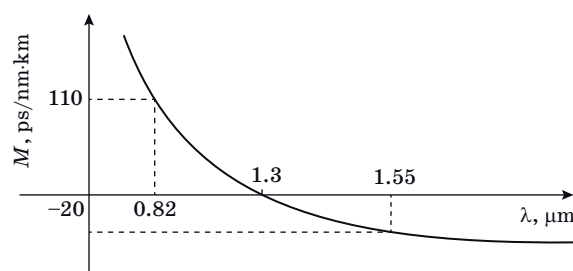
It is clearly seen that  $M = 0$  near 1300 nm, that is, here the pulse has a minimum spreading factor. In the range 1200 to 1600 nm, the material dispersion factor can be approximated by:

$$M = \frac{M_0}{4} \left( \lambda - \frac{\lambda_0^4}{\lambda^3} \right), \quad (3)$$

where  $M_0 \approx -0/095$  ps/(nm·km) and  $\lambda_0 \approx 1300$  nm (wavelength where  $M = 0$ ). At 1500 nm,  $M \approx -20$  ps/(nm·km).

For the case of *material dispersion* caused by cable material inhomogeneity along the fiber we can use the following formula (see [12, 14]):

$$\Delta\left(\frac{\tau}{l}\right) = -M\Delta\lambda. \quad (4)$$



■ Fig. 6. Dependence of dispersion properties of fiber-optic materials vs the length of optical waves  $\lambda$ , extracted from [4, 6]

For example, using an optical detector of type LED with spectral width of 20 nm (see [4]), yields a pulse spread per unit length of the transmission path inside the fiber:

$$\Delta\left(\frac{\tau}{l}\right) = -M\Delta\lambda = -(-20) \cdot 20 = 400 \text{ ps/km.}$$

*Multimode Dispersion (MMD).* Now we will discuss the modal dispersion caused by non-symmetrical distribution of the refractive index within the asymmetric fiber structure. In the case of the step-index fiber, as described above, we, following [12, 14], can obtain a pulse spread per unit length along the fiber:

$$\Delta\left(\frac{\tau}{l}\right) = \frac{n_1}{cn_2}(n_1 - n_2) = \frac{n_1}{c}\Delta. \quad (5)$$

If we account now for the fractional refractive index, we finally get that the modal pulse spread can be expressed as

$$\Delta\left(\frac{\tau}{l}\right) = \frac{n_1\Delta}{c}$$

or

$$\Delta\left(\frac{\tau}{l}\right) = \frac{n_1^2 - n_2^2}{2cn_1}. \quad (6)$$

Here, as above,  $c$  is the speed of light. The problem with pulse spreading is that it limits the information carrying capacity of the fiber. This aspect we will discuss below, where the data stream parameters of information passing the fiber optic channel will be considered.

This means that the time delay dispersion  $\tau$  of set of pulses along the fiber with the length  $l$ ,  $\Delta(\tau/l)$

can be estimated by knowledge of refraction indexes of the inner and outer cables,  $n_1$  and  $n_2$ .

In the case of modal dispersion caused by multimode propagation inside the optic fiber, a spread of information pulses at the length of an optical cable in time is given by (see [12])

$$\Delta T = \frac{ln_1^2}{cn_2}\Delta \propto \frac{ln_1}{cn_2}\Delta. \quad (7)$$

### Data stream parameters in fiber optic communication links

The problem with optical data signal spreading is that it limits the information carrying capacity of the channel [9, 10, 12, 14]. Pulses that spread, eventually overlap with neighboring pulses, creating inter-symbol interference [9–11]. This leads to transmission errors and must be avoided. The direct way to avoid this is to place pulses further apart from the transmitter. This means lowering the data rate.

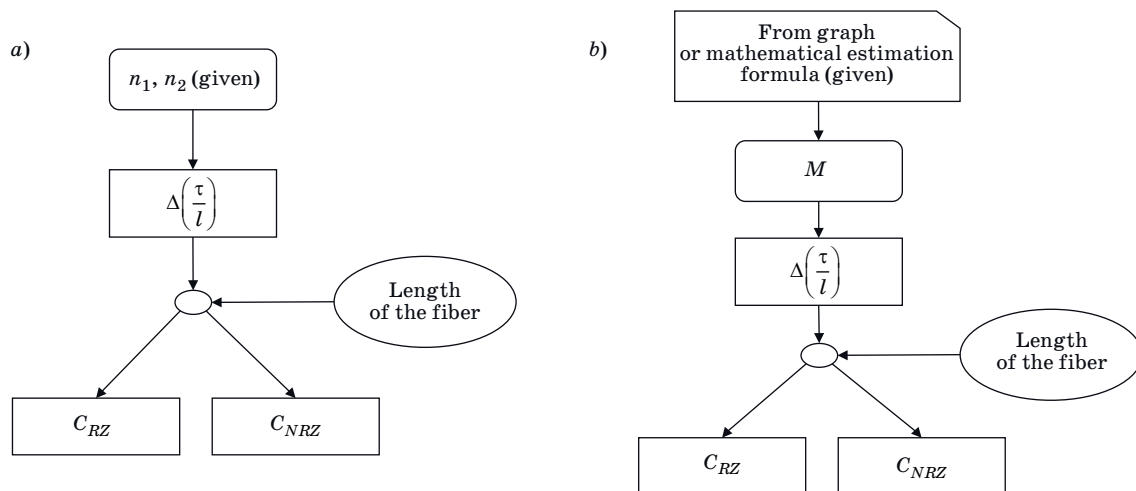
Then limitations in capacity of data flow inside the fiber depend on the type of pulses, either return-to-zero (RZ) or non-return-to-zero (NRZ) (see [14]). Thus, for RZ pulses, we get

$$C_{RZ} \times l = \frac{0.35}{\Delta(\tau/l)}.$$

Whereas, for NRZ pulses we get

$$C_{NRZ} \times l = \frac{0.7}{\Delta(\tau/l)}.$$

Using numerical data regarding material dispersion parameter  $M$ , presented above, we can also



■ Fig. 7. Diagram of the algorithm of the computation of fiber optic channel capacity in the case of multimode dispersion (a) and material dispersion  $M$  (b) along the length  $l$  of the optical cable

obtain the empirical formulas for computation of the capacity of fiber optic channels along the length  $l$  for two types of pulses, that is,

$$C_{NRZ} \times l = 1.75 \text{ (Mbit/s)} \cdot \text{km}$$

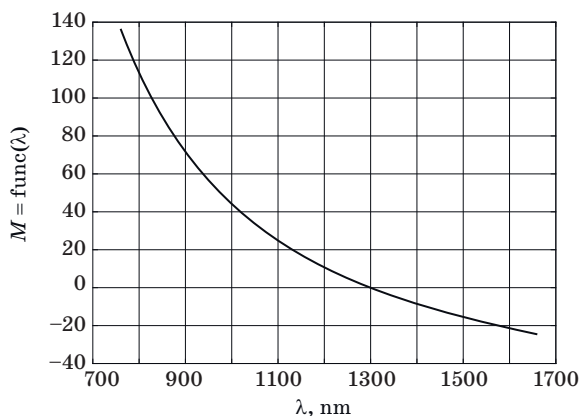
and

$$C_{RZ} \times l = 0.875 \text{ (Mbit/s)} \cdot \text{km}.$$

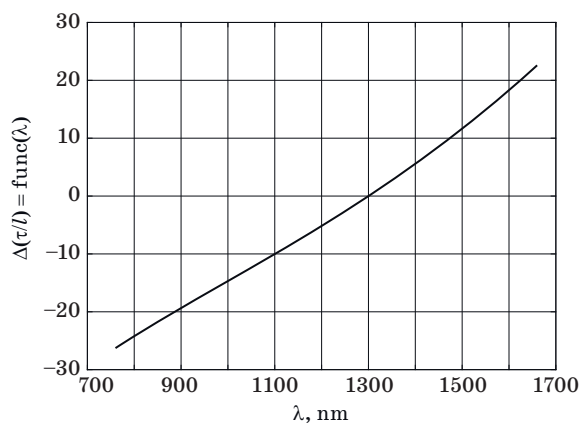
In Fig. 7, *a* and *b* the corresponding diagrams show the algorithm of computation of the capacity of the fiber optic communication links with time dispersion caused by multimode interference and by material inhomogeneity along the optical cable.

### Results of numerical simulation

In Fig. 8, the dependence of the factor of material dispersion versus the wavelength along the optic fiber [according to formula (3)] is illustrated.



■ Fig. 8. The factor of material dispersion along the optic fiber vs wavelength



■ Fig. 9. The delay along the fiber-optic channel vs wavelength along this fiber

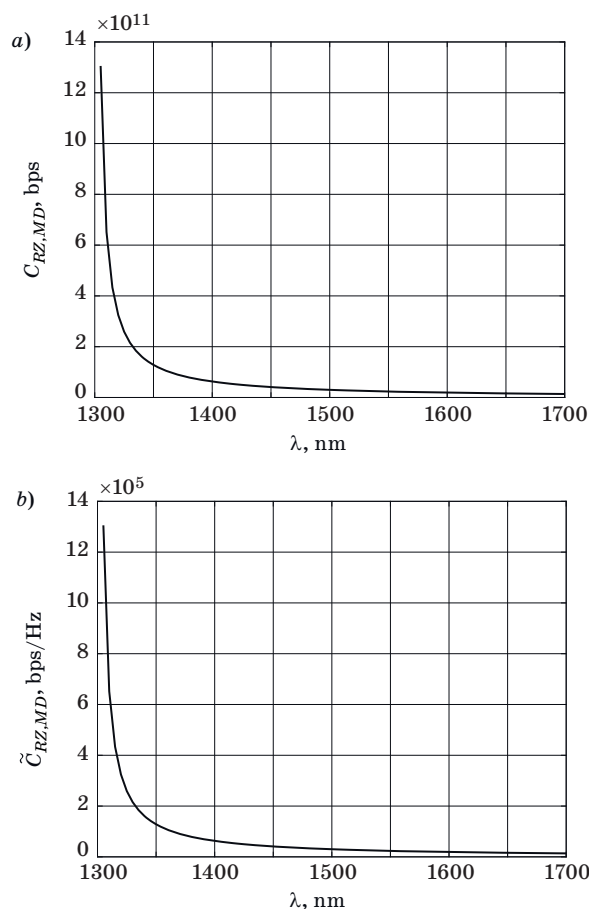
From Fig. 8 it is seen that with an increase of wavelength, the factor of material dispersion is decreased exponentially, when for a wavelength of 1300 nm this factor is zero.

In Fig. 9 the dependence of the delay along the fiber-optic channel versus the wavelength along this fiber [according to formula (4)], is illustrated.

From Fig. 9 it is seen that with an increase of wavelength, the delay is also increased almost linearly, when for a wavelength of 1300 nm this delay is zero.

In Fig. 10, *a* and *b* the dependence of the capacity and the spectral efficiency of the type RZ, of the fiber-optic channel versus the wavelength along this fiber with a length of 1 km, for material dispersion is illustrated.

From Fig. 10 it is clearly seen that with an increase of the difference between the refraction indexes of the inner and outer parts of the fiber, the capacity and the spectral efficiency of the type RZ, for material dispersion, of such a fiber optic channel is decreased exponentially. Thus, the maximum rate of data passing through such a channel also decreases exponentially.



■ Fig. 10. The capacity (a) and the spectral efficiency (b) of the type RZ, of the fiber communication link with the length of 1 km for material dispersion vs the wavelength along this fiber

In Fig. 11, *a* and *b* the dependence of the capacity and the spectral efficiency of the type NRZ, of the fiber-optic channel versus the wavelength along this fiber with a length of 1 km, respectively, for material dispersion is illustrated.

From Fig. 11 it is clearly seen that with an increase of the wavelength of an optical signal with data, propagating inside the optical cable, the capacity and the spectral efficiency of the type NRZ, for material dispersion, of such a fiber optic channel is decreased exponentially. Thus, the maximum rate of data passing through such a channel also decreases exponentially.

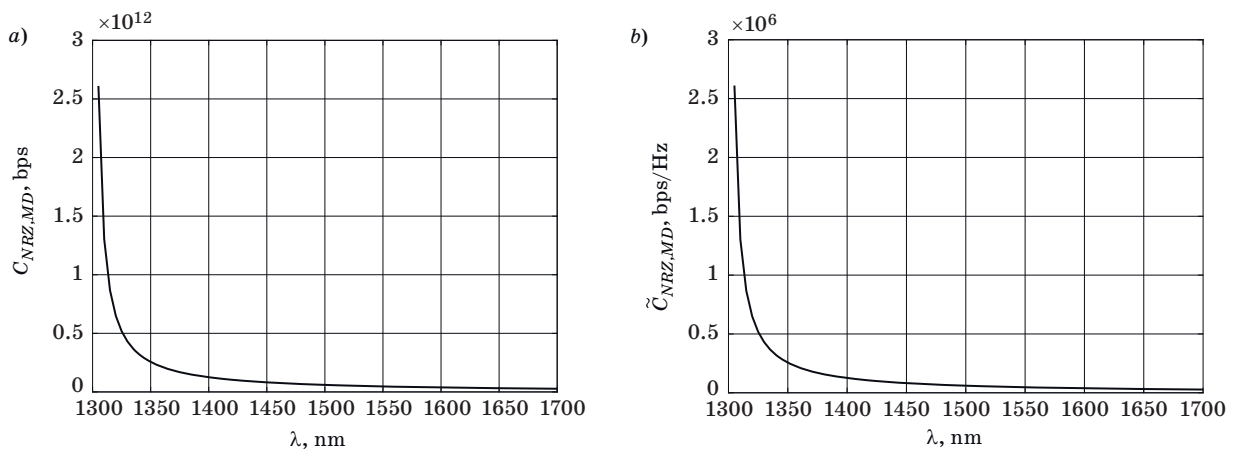
In Fig. 12, *a* and *b* the dependence of the capacity of the fiber-optic channel versus the *fractional refractive indexes difference* (FRID) of the inner and outer cables along the length of a cable of 1 km and for  $n_1 = 1.45$  [according to formulas (5), (6)], is illustrated.

From Fig. 12, *a* and *b* it is clearly seen that with an increase of the FRID of the inner and outer parts of the fiber, the broadening of pulses of such a fiber-optic channel is increased linearly.

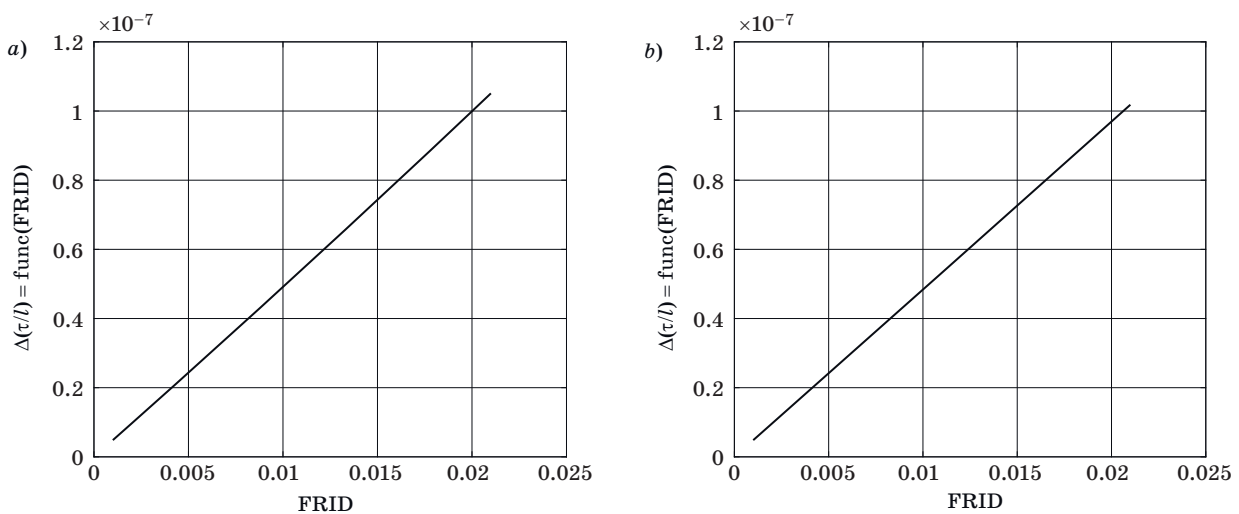
In Fig. 13 the dependence of the broadening of the pulses of information data signals along the fiber-optic channel versus the FRID of the inner and outer cables along the length of a cable of 1 km for  $n_1 = 1.45$  [according to formula (7)], is illustrated.

From Fig. 13 it is seen that with an increase of the difference between the refraction indexes of the inner and outer parts of the fiber, the broadening of pulses of such a fiber-optic channel is increased linearly.

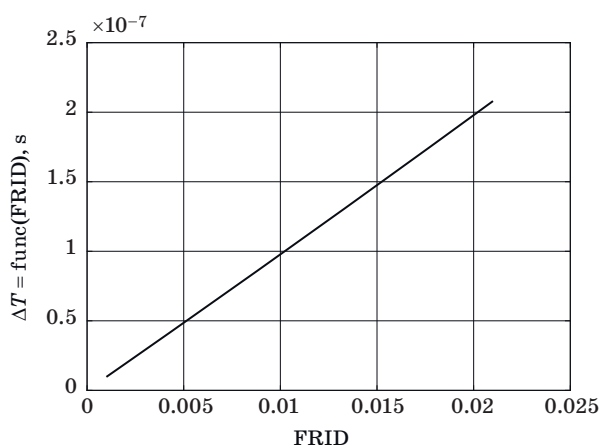
In Fig. 14, *a* and *b*, the dependence of the capacity and the spectral efficiency of the signal code of type of RZ, for multimode dispersion, of the fiber-optic channel versus the FRID of the inner and outer cables along the length of a cable of 1 km and



■ Fig. 11. The capacity (*a*) and the spectral efficiency (*b*) of the type NRZ, of the fiber communication link with the length of 1 km for material dispersion vs the wavelength along this fiber



■ Fig. 12. The delay of the fiber communication link with the length of 1 km vs the FRID of the cladding and core of the optical cable for  $n_1 = 1.45$ : *a* — formula (5); *b* — formula (6)

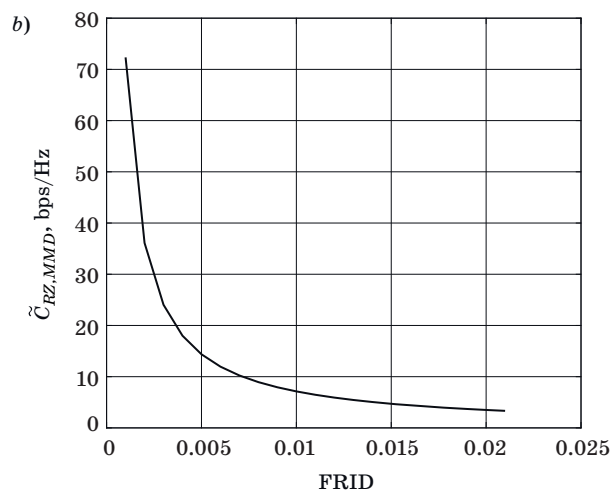
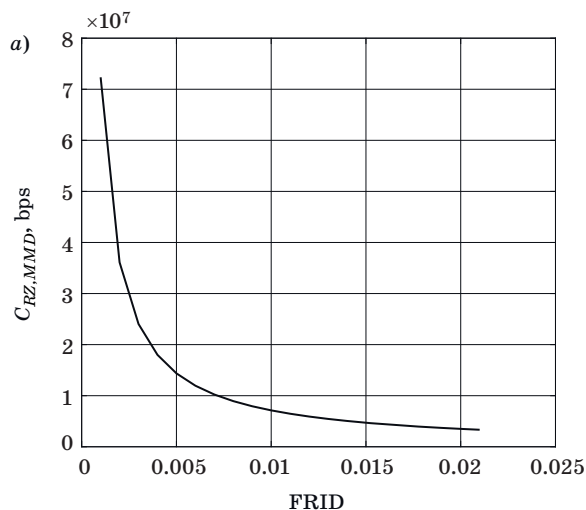


■ **Fig. 13.** The broadening of the pulses of information along the fiber with a length of 1 km vs the FRID of the cladding and core of the optical cable for  $n_1 = 1.45$

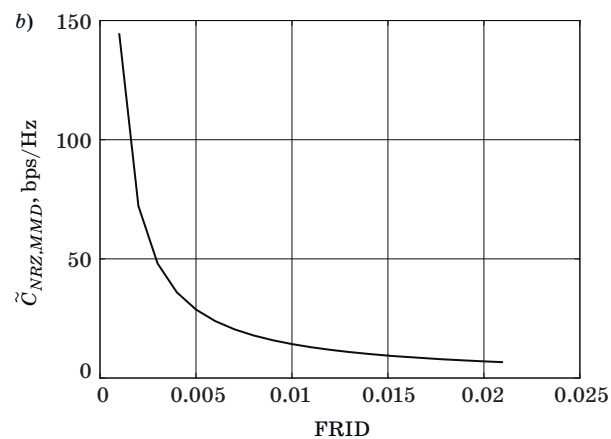
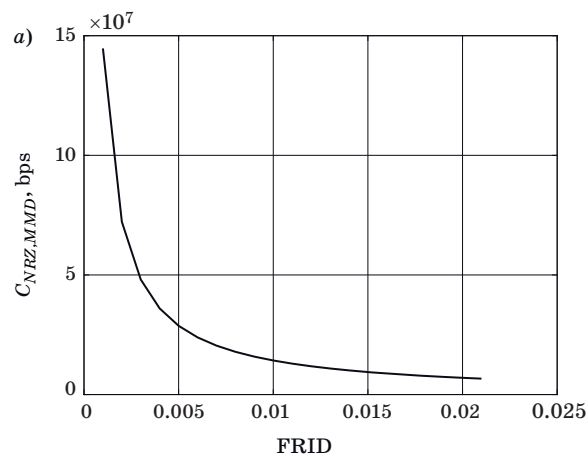
for  $n_1 = 1.45$ , for multimode dispersion [formula (5)], is illustrated.

From Fig. 14 it is clearly seen that with an increase of the difference between the refraction indexes of the inner and outer parts of the fiber, the capacity and the spectral efficiency of the RZ-type, for multimode dispersion (5), of such a fiber optic channel is decreased exponentially. Thus, the maximum rate of data passing through such a channel also decreases exponentially.

In Fig. 15, *a* and *b* the dependence of the capacity and the spectral efficiency of the signal codes of type NRZ, for multimode dispersion, of the fiber-optic channel versus the FRID of the inner and outer cables along the length of a cable of 1 km and for  $n_1 = 1.45$ , for multimode dispersion [formula (5)].

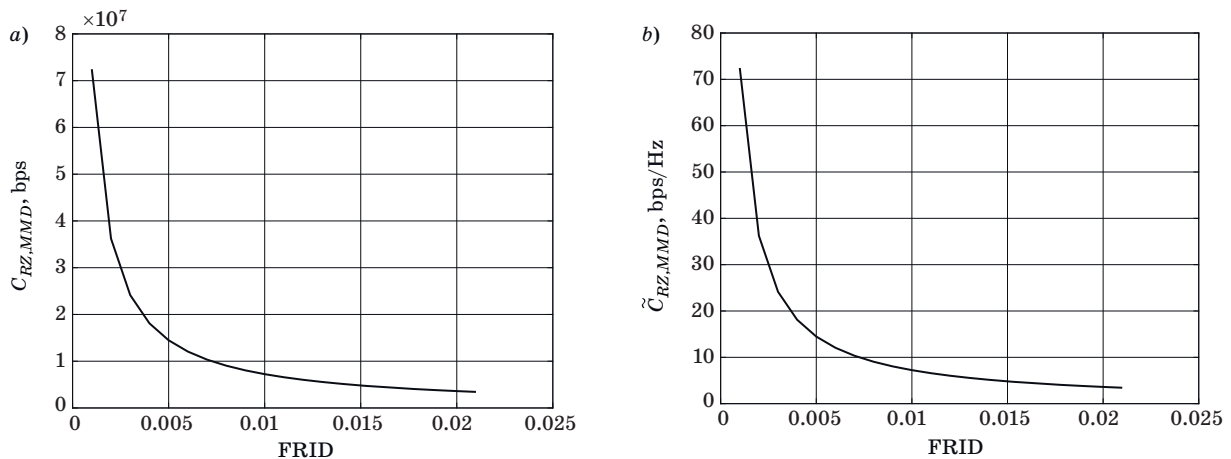


■ **Fig. 14.** The capacity (a) and the spectral efficiency (b) of the type RZ, of the fiber communication link with the length of 1 km for multimode dispersion vs FRID of the cladding and core of the optical cable for  $n_1 = 1.45$

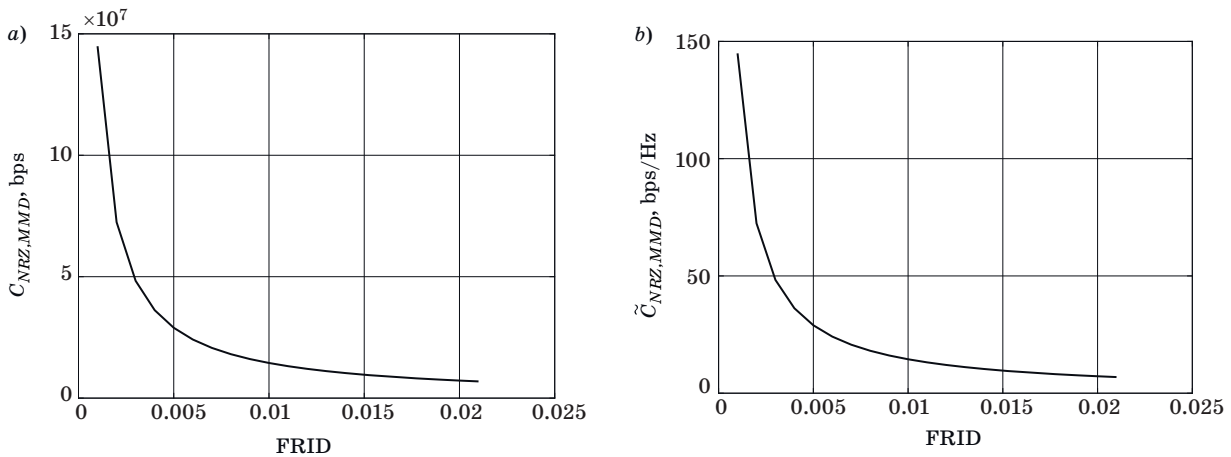


■ **Fig. 15.** The capacity (a) and the spectral efficiency (b) of the type NRZ, of the fiber communication link with a length of 1 km for multimode dispersion vs FRID of the cladding and core of the optical cable for  $n_1 = 1.45$





■ Fig. 16. The capacity (a) and the spectral efficiency (b) of the type RZ, of the fiber communication link with a length of 1 km for multimode dispersion vs FRID of the cladding and core of the optical cable for  $n_1 = 1.45$



■ Fig. 17. The capacity (a) and the spectral efficiency (b) of the type NRZ, of the fiber communication link with a length of 1 km for multimode dispersion vs FRID of the cladding and core of the optical cable for  $n_1 = 1.45$

From Fig. 15 it is clearly seen that with an increase of the difference between the refraction indexes of the inner and outer parts of the fiber, the capacity and the spectral efficiency of the NRZ-type signal codes, for multimode dispersion (5), of such a fiber optic channel is decreased exponentially. Thus, the maximum rate of data passing through such a channel also decreases exponentially.

In Fig. 16, a and b the dependence of the capacity and the spectral efficiency of the type RZ, for multimode dispersion, of the fiber-optic channel versus the fractional refractive indexes difference FRID of the inner and outer cables along the length of a cable of 1 km and for  $n_1 = 1.45$ , for multimode dispersion [(formula (6))], is illustrated.

From Fig. 16 it is clearly seen that with an increase of the difference between the refraction indexes of the inner and outer parts of the fiber, the capacity and the spectral efficiency of the RZ-type

signal codes, for multimode dispersion (6, of such a fiber optic channel is decreased exponentially. Thus, the maximum rate of data passing through such a channel also decreases exponentially.

In Fig. 17, a and b the dependence of the capacity and of the spectral efficiency of the type NRZ, for multimode dispersion, of the fiber-optic channel versus the FRID of the inner and outer cables along the length of the cable of 1 km and for  $n_1 = 1.45$ , for multimode dispersion [(formula (6))], is illustrated.

From Fig. 17 it is clearly seen that with an increase of the difference between the refraction indexes of the inner and outer parts of the fiber, the capacity and the spectral efficiency of the NRZ-type signal codes, for multimode dispersion (6), of such a fiber optic channel is decreased exponentially. Thus, the maximum rate of data passing through such a channel also decreases exponentially.

## Summary

Theoretical analysis and the corresponding computer simulation using the MATLAB utility have shown that:

1. Depending on the wavelength of optical signal propagating inside the fiber-optic communication channel, the material dispersion index is decreased exponentially with an increase of the signal wavelength.

2. At the same time, with an increase of the wavelength of optical signal passing through the fiber optic channel, the delay spread (e. g., widening) of the resulting optical signal inside the cable increases linearly.

3. The material time-dispersion parameter along the fiber optic cable increases linearly with an

increase of the difference between the refraction indexes of the inner and outer parts of the fiber, called fractional refractive indexes difference (FRID).

4. The exponential decrease of the signal data flow of fiber-optic channels is observed with FRID both for NRZ- and RZ-types of codes inside the data flow.

5. The multimode time dispersion depends significantly on the difference between the refraction indexes of the inner and outer parts of the fiber, and with an increase of FRID, it increases linearly.

6. For both types of signal codes, NRZ and RZ, exponential decrease of the channel capacity and spectral efficiency is observed — the multimode dispersion — depends on the difference between the refraction indexes of the inner and outer parts of the fiber and on the increase of the length of the channel (e. g., fiber cable).

## References

- Dudley J. M., and Taylor J. R. *Supercontinuum generation in optical fibers*. London, Cambridge University Press, 2010. 167 p.
- Shu Namiki, Takayuki Kurosu, Ken Tanizawa, Stephane Petit, Mingyi Gao, Junya Kurumida. Controlling optical signals through parametric processes. *IEEE Journal of Selected Topics in Quantum Electronics*, 2012, vol. 18, no. 2, pp. 717–725.
- Okuno T., Hirano M., Nakanishi T., and Onishi M. Highly-nonlinear optical fibers and their applications. *SEI Tech. Rev.*, 2006, no. 62, pp. 34–40.
- Wandel Marie, and Kristensen Poul. Fiber designs for high figure of merit and high slope dispersion compensating fibers. *J. Opt. Fiber. Commun.*, 2006, vol. 3, no. 1, pp. 25–60.
- Poletti F., Feng X., Ponzio G. M., Petrovich M. N., Loh W. H., Richardson D. All-solid highly nonlinear single mode fibers with a tailored dispersion profile. *Optics Express*, 2011, vol. 19, no. 1, pp. 66–80.
- Shuai C., Gao C., Nie Y., and Peng S. Performance improvement of optical fiber coupler with electric heating versus gas heating. *Appl. Opt.*, 2010, vol. 49, pp. 4514–4519.
- Jasion G. T., Shrimpton J. S., Chen Y., Bradley T., Richardson D. J., and Poletti F. MicroStructure Element Method (MSEM): viscous flow model for the virtual draw of microstructured optical fibers. *Optics Express*, 2015, vol. 23(1), pp. 312–329.
- Kostecki R., Ebendorff-Heidepriem H., Warren-Smith S. C., and Monroe T. M. Predicting the drawing conditions for microstructure optical fiber fabrication. *Optical Materials Express*, 2014, vol. 4, no. 1, pp. 29–40.
- Aparna A. Nair, Sudheer S. K., and Jayaraju M. Analysis of optical characteristics for photonic crystal fiber at small core diameters. *International Journal of Engineering and Advanced Technology (IJEAT)*, 2014, vol. 3, iss. 4, pp. 377–380.
- Filipenko A. I., Ponomarjova A. V. Modern state of the problem of the design-geometric parameters of micro structured optic fibers control. *Radiotekhnika*, 2008, no. 154, pp. 102–107 (In Russian).
- Mishra S. S., and Singh V. K. Comparative study of fundamental properties of honey comb photonic crystal fiber at 1.55  $\mu\text{m}$  wavelength. *Journal of Microwaves, Optoelectronics and Electromagnetic Applications*, 2011, vol. 10, no. 2, pp. 343–354.
- Palais J. C. *Optical Communications*. In: *Engineering Electromagnetics Applications*. Ed. by R. Bansal. New York, Taylor and Frances, 2006.
- Tiker A., Yarkoni N., Blaunstein N., Zilberman A., Kopeika N. Prediction of data stream parameters in atmospheric turbulent wireless communication links. *Applied Optics*, 2007, vol. 46, no. 2, pp. 190–199.
- Blaunstein N. Sh., Krouk E. A., and Sergeev M. B. *Opticheskaya svyaz': optovolokonnyya, atmosfernaya* [Optical Communication: Fiber Optic, Atmospheric]. Saint-Petersburg, Sankt-Peterburgskij gosudarstvennyj universitet aerokosmicheskogo priborostroyeniya Publ., 2016. 286 p. (In Russian).

УДК 621.371

doi:10.31799/1684-8853-2019-3-94-104

**Оптические сигналы в оптоволоконных линиях связи с федингом**И. Джувилер<sup>а</sup>, PhD, старший преподаватель, orcid.org/ 0000-0002-0669-7828И. Бронфман<sup>а</sup>, ассистент, orcid.org/ 0000-0001-6195-069XН. Блаунштейн<sup>б</sup>, доктор физ.-мат. наук, профессор, orcid.org/ 0000-0003-2945-9379, nathan.blaunstein@hotmail.com<sup>а</sup>Технический колледж им. Сами Шамуна, ул. Жаботинского, 84, Ашдод, 77245, Израиль<sup>б</sup>Негевский университет им. Бен-Гуриона, П.О.Б. 653, Бен-Гуриона ул., 1, Беэр-Шева, 74105, Израиль

**Введение:** исследование параметров сигналов в оптоволоконных каналах связи и дисперсионных свойств оптических сигналов, обусловленных неоднородностью материала и многомодовым характером распространения оптических сигналов в данных типах проводной связи, является актуальной проблемой для создания современных систем проводной связи 4-го и 5-го поколений, подверженных федингу, вызванному вышеупомянутым выше фактором, с большой скоростью в условиях многочисленного контингента пользователей. **Цель:** исследование характера многомодовой дисперсии на основе анализа распространения волноводных оптических волн вдоль оптоволоконного с различным профилем показателя рефракции внутреннего оптического кабеля относительно внешней оболочки, а также дисперсионных свойств оптоволоконного за счет неоднородности материала оболочки вдоль длины кабеля для двух типов сигналов в последовательности кодов, передаваемых через оптический кабель: возвратных и невозвратных к нулю кодов. **Методы:** дисперсионные свойства многомодового распространения внутри оптоволоконного кабеля проанализированы введением трехмерной модели распространения оптической волны в заданной направляющей структуре. Эффекты многомодовой дисперсии и материальной дисперсии, вызывающих «уширение» времени запаздывания оптических сигналов вдоль кабеля, исследовались аналитически и численно. **Результаты:** получены и проиллюстрированы свойства временной дисперсии двух видов оптоволоконных структур: с пошаговым и степенным профилем показателя преломления, — вызванной многомодовым (многолучевым) распространением и неоднородностью материала вдоль кабеля, а именно интерференцией мод, распространяющихся по оптическому кабелю, и нарушением зеркального отражения мод от стенок кабеля на неоднородностях материала стенок. Их воздействие на емкость и спектральную эффективность потока сигналов с данными, пропускаемого подобной направляющей структурой, проиллюстрировано для произвольных индексов рефракции внутреннего (стержень) и внешнего (оболочка) элементов оптического кабеля. Применен новый метод нахождения и оценки эффектов временной дисперсии оптических сигналов, распространяющихся в различных видах оптоволоконных структур. Предложен алгоритм оценки потерь в спектральной эффективности, измеряемой в битах на секунду на герц на один километр, вдоль длины кабеля для произвольного представления кодовых сигналов в потоке данных, невозвратных к нулю и возвратных к нулю. Все практические проверки были проиллюстрированы с использованием программы MATLAB.

**Ключевые слова** — емкость, оболочка, стержень, уширение задержки оптических импульсов, дисперсионные кривые, дисперсионные диаграммы оптических мод, оптоволоконно, кабель со степенным профилем рефракции, многомодовая дисперсия, линейно-поляризационные моды, фактор материальной дисперсии, многомодовая временная дисперсия, невозвратный к нулю код, численная апертура, оптические моды кабеля, индекс рефракции, возвратный к нулю код, условие существования единственной моды, спектральная эффективность, кабель с пошаговым профилем рефракции.

**Для цитирования:** Juwiler I., Bronfman I., Blaunstein N. Optical data signals in fiber optic communication links with fading. *Информационно-управляющие системы*, 2019, № 3, с. 94–104. doi:10.31799/1684-8853-2019-3-94-104

**For citation:** Juwiler I., Bronfman I., Blaunstein N. Optical data signals in fiber optic communication links with fading. *Informatsionno-upravliaiushchie sistemy* [Information and Control Systems], 2019, no. 3, pp. 94–104. doi:10.31799/1684-8853-2019-3-94-104